1521-0103/382/1/11–20$35.00
THE JOURNAL OF PHARMACOLOGY AND EXPERIMENTAL THERAPEUTICS

dx.doi.org/10.1124/jpet.121.001058
J Pharmacol Exp Ther 382:11–20, July 2022

The Journal of PHARMACOLOGY And Experimental Therapeutics

Sodium Pentobarbital Suppresses Breast Cancer Cell Growth Partly via Normalizing Microcirculatory Hemodynamics and Oxygenation in Tumors

Qin Wang,[1] Xueting Liu,[1] Bingwei Li, Xiaojie Yang, Wenbao Lu, Ailing Li, Hongwei Li, Xiaoyan Zhang, and Jianqun Han

Microhemodynamics Laboratory, Institute of Microcirculation (Q.W., X.Y., H.Q.), Laboratory of Microvascular Biopathology, Institute of Microcirculation (X.L., X.Z.), and Institute of Microcirculation (B.L., W.L., A.L., H.L.), Chinese Academy of Medical Sciences & Peking Union Medical College, Beijing, China

Received December 17, 2021; accepted April 26, 2022

ABSTRACT

Breast cancer remains the leading cause of cancer-related death among women worldwide. Sodium pentobarbital was found to play an inhibitory role in glioma growth in rats. In this study, we aimed to evaluate the effects of sodium pentobarbital on breast cancer growth both in vitro and in vivo, and its impacts on the microcirculatory changes on both skin and tumor surface in mice bearing subcutaneous xenograft. Cell counting assay was used to assess the antiproliferative effect of sodium pentobarbital on MDA-MB-231 breast cancer cells. Subcutaneous xenograft model was established to study the role of sodium pentobarbital on in vivo tumor growth. Speed-resolved blood perfusion, hemoglobin oxygen saturation (SO_2, %), total hemoglobin tissue concentration (ctTHb, μM), and red blood cell (RBC) tissue fraction (%) were examined simultaneously by using enhanced perfusion and oxygen saturation system to investigate the effects of sodium pentobarbital on microcirculatory hemodynamics and oxygenation. Sodium pentobarbital suppressed breast tumor growth both in vitro and in vivo. Cutaneous blood flux in nutritive capillaries with low-speed flow was significantly increased in tumor-bearing mice, and high-dose sodium pentobarbital treatment cause a reduction in this low-speed blood flux, whereas sodium pentobarbital therapy caused an elevated blood flux in larger microvessels with mid and high speed in a dose-dependent manner. Different doses of sodium pentobarbital exerted different actions on SO_2, ctTHb, and RBC tissue fraction. Collectively, the inhibitory effect of sodium pentobarbital on breast tumor growth was at least partly associated with its ability to normalize microcirculatory hemodynamics and oxygenation in tumors.

SIGNIFICANCE STATEMENT

This study is the first to demonstrate the inhibiting effect of sodium pentobarbital on breast cancer growth both in vitro and in vivo, and such an inhibition was at least partly associated with its ability to normalize microcirculatory hemodynamics and oxygenation in tumors.

Introduction

Breast cancer is the most common cancer among women, accounting for 24% of total new diagnoses, and is the leading cause of cancer-related death among women worldwide (Sung et al., 2021). The standard of treatment of breast cancer involves a combination of surgery, chemotherapy, radiation therapy, and targeted therapy. However, breast cancer surgery can affect quality of life, fatigue, and cognition in patients over the age of 65 years (Harrison et al., 2021). After breast-conserving surgery of hormone receptor-positive (HR^+) breast cancer, standard treatments such as radiation therapy and endocrine therapy can easily cause treatment-related toxicities and noncancer-related death for elderly patients (Savard et al., 2021). Chemotherapy drug such as taxanes can cause polyneuropathy (Park et al., 2013; Ilhan et al., 2017; Ciruelos et al., 2019). Effects of targeted drugs for triple-negative breast cancer are limited, and lapatinib showed drug resistance for human epidermal growth factor receptor 2 (HER2)-positive breast cancer therapy (Sang et al., 2021). There is an urgent need to continue to explore new drugs with antitumor potential for breast cancer.

Sodium pentobarbital (P. Barbital) is a fast-acting central depressant acting via γ-aminobutyric acid (GABA) receptors (Mohamed et al., 2020), which is mostly used as an anesthetic agent in animal experiments (Matsuura and Downie, 2000; Tanioka et al., 2020; Xu et al., 2020; Barry et al., 2021). Oral pentobarbital has also been the preferred sedative in pediatric echocardiography in several pediatric departments (Warden

This research was funded by the Institute of Microcirculation, Peking Union Medical College Fundamental Research Fund [Grant/Award WXH2020-02].
The authors declare no conflict of interest.
[1]Q.W. and X.L. contributed equally to this work
dx.doi.org/10.1124/jpet.121.001058.

ABBREVIATIONS: ctO_2Hb, oxygenized hemoglobin concentration; ctTHb, total hemoglobin tissue concentration; DRS, diffuse reflectance spectroscopy; EPOS, enhanced perfusion and oxygen saturation; LDF, laser Doppler flowmetry; P. Barbital, sodium pentobarbital; RBC, red blood cell; Sk, tumor skin; SO_2, hemoglobin oxygen saturation; Ts, tumor surface.

et al., 2010; Miller et al., 2018). Notably, some studies reported that phenobarbital exerted inhibitory effects on the development of gliomas in Wistar Furth (WF) rats treated neonatally with N-ethyl-N-nitrosourea (Naito et al., 1985). Consistently, an in vitro study demonstrated that pentobarbital is capable of inhibiting proliferation and migration of malignant glioma cells by arresting cell cycle and interfering microtubule (Xie et al., 2009). However, little is known about the effect of pentobarbital on other types of tumors, including breast cancer.

Blood flow is a major driving factor for metabolism and oxygenation in tumor tissues, which, in turn, may have an impact on the effectiveness of some cancer therapies. Tumor blood vessels usually exhibit anomalous morphology characterized by irregular diameters, immature vessel walls, and increased vessel tortuosity and permeability, which lead to abnormal microcirculatory blood flow (MBF) (Andleeb et al., 2021). Thus, tumor tissue oxygenation and microcirculatory blood flow are crucial indices for detecting tumor growth and can be used to monitor alterations within the tumor microenvironment and predict neoadjuvant chemotherapy response in both preclinical and clinical research (Tromberg et al., 2016; Jing et al., 2019; Koch et al., 2020). There are numerous techniques to measure blood blow and microcirculatory oxygen profiles within tumors, respectively. With regard to blood flow, conventional laser Doppler flowmetry (LDF) is a standard technique for monitoring blood flow noninvasively. LDF provides an indicator of the concentration and velocity of moving blood cells within a region of limited depth, presented in arbitrary units (Smith et al., 2019). Although this technique is of great value in physiologic and medicine research, it has not been capable of giving microvascular perfusion in absolute units (Roustit and Cracowski, 2012). In this study, we employed a newly developed equipment called EPOS (enhanced perfusion and oxygen saturation) system, which integrates diffuse reflectance spectroscopy (DRS) and LDF to simultaneously provide absolute measures of both microcirculatory hemodynamics such as velocity-resolved perfusion separated into three speed regions [0–1 mm/s, 1–10 mm/s, and above 10 mm/s (% mm/s)] and microcirculatory oxygen profiles, including hemoglobin oxygen saturation (SO_2, %), red blood cell (RBC) tissue fraction (%) and oxygenized and reduced hemoglobin tissue concentration (μM) (Fredriksson et al., 2013; Jonasson et al., 2015). Owing to its accessibility, cutaneous microcirculation has emerged as a typical vascular bed for the evaluation of systemic microvascular function and dysfunction (Deegan and Wang, 2019) under various pathologic conditions such as diabetes (Feng et al., 2018), hypertension (Concistrè et al., 2020), Raynaud's phenomenon (Anderson et al., 2004), and cardiovascular diseases (Shamim-Uzzaman et al., 2002; Agarwal et al., 2012), suggesting the importance of the assessment cutaneous microcirculation in patients to elaborate the underlying pathophysiological mechanisms or to be used as a predictor of treatment response. There are few studies focused on the changes of cutaneous microcirculation in cancer patients (Hsiu et al., 2018; Pedanekar et al., 2019).

Thus, in the present study, we aimed to investigate the potential effects of sodium pentobarbital on the growth of breast cancer both in vitro and in vivo and to measure sodium pentobarbital–induced microcirculatory hemodynamics and oxygenation changes in tumor.

Materials and Methods

Cell Culture and Treatment. MDA-MB-231 breast cancer cell line was obtained from National Infrastructure of Cell Line Resource (NICR) (Institute of Basic Medical Science, Chinese Academy of Medical Science and Peking Union Medical College, Beijing, China). The authentication of MDA-MB-231 cell line was performed by using short tandem repeat (STR) typing test (Shanghai Biowing Biotechnology Co. Ltd., Shanghai, China). STR typing profiles showed that 100% matched cell line was found in the DSMZ data bank, the name of cell line was MDA-MB-231, and no multiple alleles were found. Cells were maintained in Dulbecco's modified Eagle's medium (DMEM) (Gibco) supplemented with 10% fetal bovine serum (Gibco) in a humidified incubator with 5% CO_2 at 37°C. For cell treatment, MDA-MB-231 cells were plated in a 12-well plate at a density with 60% confluence and were treated with 0.15, 0.3, 0.6, 1.5 and 3.0 mg/ml sodium pentobarbital (cat# P3761-5G; Sigma-Aldrich, St. Louis, MO) for 40 hours.

Cell Counting Assay. Cell counting assay was conducted by experienced researchers. Briefly, MDA-MB-231 cells were seeded into 96-well plates at a density of 5×10^3 cells per well in 50 μl DMEM for 24 hours until 60% confluence. Cells were treated with a series of concentrations of P. Barbital (0.15, 0.3, 0.6, 1.5 and 3.0 mg/ml) for 8, 16, 24, 32, and 40 hours and were then counted using an IncuCyte Zoom Live-Cell Imaging System (2015A; Essen Bioscience, Ann Arbor, MI).

In Vivo Tumor Formation Assay. Animal care and experimental protocols were in accordance with the Institute for Laboratory Animal Research *Guide for the Care and Use of Laboratory Animals* (8th ed.) (National Research Council, 2011) and were approved by the Institutional Animal Care and Use Committee at the Institute of Microcirculation, Chinese Academy of Medical Sciences (CAMS). Xenograft model was established by experienced laboratory technicians. Six-week-old female BALB/c nude mice (CAnN.Cg-*Foxn1*^{nu}/Crl; the 1bp (G) deletion of exon 3 of Foxn1 gene on chromosome 11 causes frameshift mutation and the introduction of a stop codon before extraction, leading to premature termination of protein translation) were provided by SPF (Beijing) Biotechnology Co., Ltd. (Beijing, China) and were housed five per cage for 5 days before injection at 24 ± 1°C in a 55% ± 5% humidified atmosphere under a 12h/12h light/dark cycle; mice had free access to regular diet (Rat & Mouse Growth and Reproduction Formula Feed; Beijing Keao Xieli Feed Co., Ltd., Beijing, China) and drinking water. Approximately 5×10^6 cells at exponential growth stage suspended in 100 μl Matrigel (BD) were inoculated into armpit of each nude mouse. Furthermore, all mice were randomly divided into four groups when tumor volume reached 80–100 mm^3: control and 5, 25, and 50mg/kg per day P. Barbital groups. Each group had six mice. Control or test P. Barbital (5, 25, or 50mg/kg per day) were injected subcutaneously around the tumor for 2 consecutive weeks. Calipers were used to measure the length and width of tumor, and tumor volumes were calculated according to the following formula: tumor volume = (length × width^2)/2.

Equipment for Measuring Microcirculatory Hemodynamics and Oxygen Profiles in Tumor. In the present study, we used the PeriFlux 6000 EPOS system (Perimed AB, Järfälla, Stockholm, Sweden), which successfully integrates laser Doppler flowmetry (LDF) and diffuse reflectance spectroscopy (DRS) to accurately measure blood perfusion and oxygen saturation in the microcirculation. The principal advantage of this new technique is that it measures blood perfusion in absolute units, not only qualitatively as when using a standard laser Doppler (Jonasson et al., 2015, 2017). Furthermore, it separates different velocity regions within the blood flow termed speed-resolved perfusion. For instance, it is able to distinguish slow nutritive blood flow, which is of great importance for all living cells in the body, from faster flow that is only responsible for transportation (Jonasson et al., 2019). Additionally, it can be used to evaluate the association between flow speed and red blood cell (RBC) oxygen saturation, revealing information about oxygen delivery and uptake into the surrounding tissue. To estimate the microcirculatory parameters, a unique model-based analysis of multimodal measurements is

employed. The multilayered tissue model is adapted to the measured signals in real time, and the following parameters are obtained from the adapted model: oxygen saturation (SO_2, %); red blood cell (RBC) tissue fraction [gram RBC/100-g tissue (%); oxygenized, reduced, and total hemoglobin tissue concentration (μM)]; and speed-resolved perfusion: gram RBC/100-g tissue × mm/s (% RBC × mm/s) (three different speed regions: <1 mm/s, 1–10 mm/s, and >10 mm/s).

Measurement Protocols. After acclimatizing for 15 minutes in an experimental room with an ambient temperature of 24 ± 1°C (mean ± S.D.) and 50%–70% humidity, the tumor-bearing mice were anesthetized with 2% inhaled isoflurane (RWD Life Science, Shenzhen, China) in a 50% mixture of oxygen using a small animal anesthesia machine (Midmark, Dayton, Ohio). Then, mice were placed in a supine position on a heating pad with continuous inhalation of isoflurane. The probe was placed upon the tumor skin (Sk) steadily by a probe holder (PLT1; Moor Instruments) after the skin was disinfected with 75% ethanol. Researchers measuring microcirculatory hemodynamics and oxygen profiles were trained by technical support from Perimed Technology (Beijing, China) Co., LTD. The microcirculatory measurements were performed on tumor skin. After the skin was peeled off, the blood perfusion on the exposed tumor surface (Ts) was also measured using the same method. At the end of experiments, mice were euthanized by CO_2 inhalation.

Statistical Analysis. Continuous variables are presented as mean ± S.D. and categorial variables as percentages. SPSS 21.0 version software (SPSS Inc., Chicago, IL) was used for data statistical analysis. Two-tailed Student's t test was used for two-group comparison, and one-way ANOVA analysis was used for statistical comparisons among multiple groups. Figures were generated by using the GraphPad Prism (version 8.0.2; GraphPad Software, San Diego, CA). $P < 0.05$ was considered as statistical significance.

Results

Sodium Pentobarbital Suppressed Tumor Cell Proliferation In Vitro. As shown in Fig. 1, compared with the control group, P. Barbital treatment induced decreased tumor cell viability in a time- and dose-dependent manner. Under normal conditions (control group), MDA-MB-231 cells grew quickly; cell number doubled at 16 hours and increased to four times after 40-hour treatment. Low dose (0.15 mg/ml) P. Barbital exposure slightly suppressed cell viability, demonstrated by the fact that cell number only doubled after 40-hour P. Barbital treatment. However, cell viability was obviously suppressed when exposure dose increased to 0.3–3.0 mg/ml. The number of living cells decreased to about 64% in 0.3 mg/ml group and 26% in 0.6 mg/ml group after 40-hour treatment. In the highest-dose P. Barbital (3.0 mg/ml) group, after 8 hours of treatment, there were very few living cells (about 4%), and there were no living cells at 16 hours. These data indicate that sodium pentobarbital suppresses the viability of breast cancer cells in vitro.

Sodium Pentobarbital Inhibited Tumor Growth In Vivo. The effects of P. Barbital at various doses on tumor growth in vivo were determined in a subcutaneous xenograft assay using the MDA-MB-231 cells. Our results showed that P. Barbital led to a significant reduction of tumor burden in a concentration-dependent manner and that the average tumor weight was reduced significantly after 2 weeks of 50 mg/kg P. Barbital injection compared with the control group (48.64 mg vs. 1117.06 mg) (Fig. 2C). Consistently, the tumor volume in the low-dose P. Barbital group (5 mg/kg) was similar to that in the control group after 1 week of treatment and then grew slowly from the 10 days

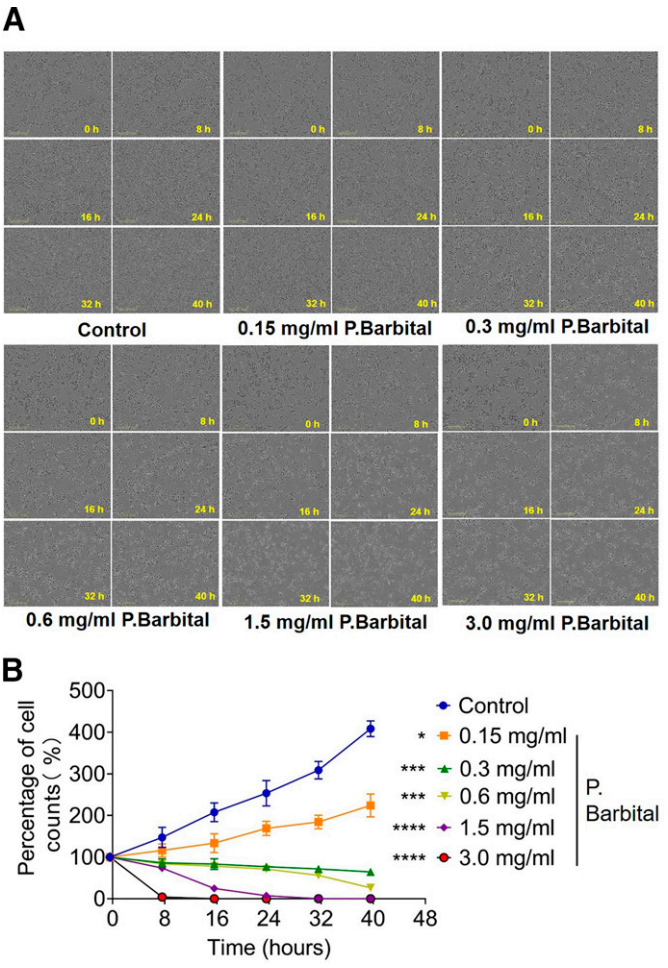

Fig. 1. Sodium pentobarbital inhibited the proliferation of breast cancer cells in vitro. (A) Equal amounts of MDA-MB-231 breast cancer cells were treated with 0.15, 0.3, 0.6, 1.5, and 3.0 mg/ml of P. Barbital at different time points, respectively. Images represent cells under light microscope. Bar: 300 μm. (B) Cell number of (A) was determined by cell counting assay using an IncuCyte Zoom Live-Cell Imaging System, and proliferation rate of P. Barbital was expressed as a fold of cell counts at 0 hours. ****$P \leq 0.0001$; ***$P \leq 0.001$; *$P \leq 0.05$ vs. control group.

after P. Barbital injection compared with the controls. In the medium dosage group (25 mg/kg), the volume of tumors was no more than 100 mm^3 throughout the observation period. In the high dose group (50mg/kg), the average tumor volume shrank to under 30 mm^3 (Fig. 2, A and B). Therefore, these findings explicitly point out that sodium pentobarbital may have a role of inhibiting tumor growth.

Effect of Different Concentration of Sodium Pentobarbital on Speed Resolved Perfusion on Tumor Skin and Tumor Surface. In the present study, we employed the newly developed EPOS system, which enables the effects in capillaries (low-speed flow) to be differentiated from those in larger microvascular vessels (high-speed flow) such as venules and arterioles, using the velocity-resolved quantitative measure to monitor microcirculatory blood flow for the first time in tumor. This system has already been used in determining the microcirculatory velocity distribution in patients with type 2 diabetes (Fredriksson et al., 2010). Analysis of association between flow velocity and vessel type may offer novel insights into the microvascular function.

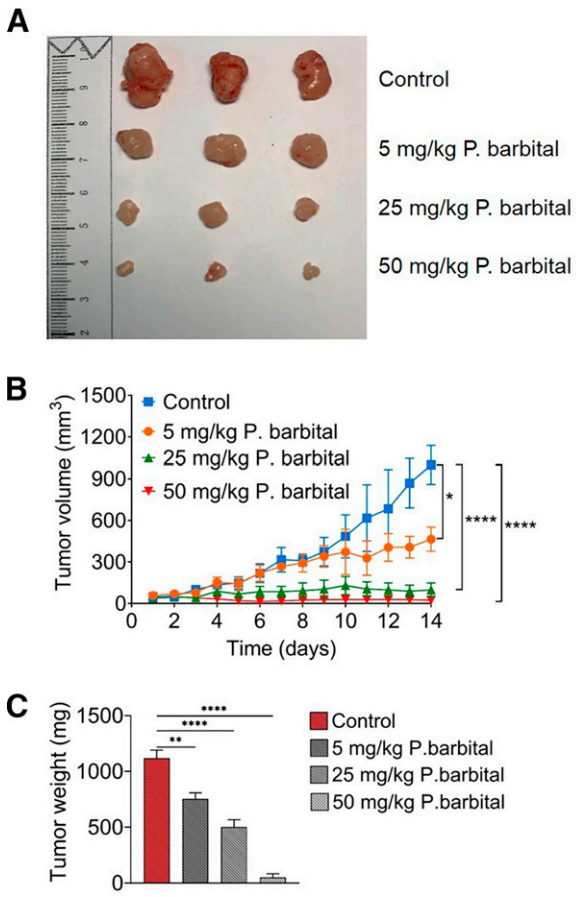

Fig. 2. Sodium pentobarbital suppressed tumor growth in vivo in a time- and dose-dependent manner. (A) Morphologic characteristics of xenograft tumors from control and 5, 25, and 50mg/kg P. Barbital groups. (B) The effect of P. Barbital on tumor growth was investigated in a subcutaneous tumor model and tumor growth was expressed as a tumor volume. Data points represent the mean ± S.D. ***$P \leq 0.001$; **$P \leq 0.01$; *$P \leq 0.05$ vs. control group. (C) Changes in tumor growth rate were also reflected by final tumor weights after 2 weeks of P. Barbital treatment. Data represent the mean ± S.D. ****$P \leq 0.0001$; *$P \leq 0.05$ vs. control group.

As Figs. 3A and 4A (left) presented, an increased blood flux occurred in low-speed regions (<1 mm/s) on tumor skin (Sk) compared with that in control skin ($P < 0.0001$), and the lowest dose (5 mg/kg) of P. Barbital treatment remarkably elevated the blood flux in the low-speed region on tumor skin ($P < 0.0001$); however, when exposure dose of P. Barbital increased to 10 times (50 mg/kg), the blood flux in the low-speed region reduced significantly on tumor skin ($P < 0.0001$). With regard to perfusion in the mid- (1–10 mm/s) and high-speed (>10 mm/s) regions, a large decrease was observed on tumor skin compared with the control skin ($P < 0.0001$ in both mid- and high-speed regions) and P. Barbital stimulation significantly increased the blood flux in the mid- and high-speed regions in a concentration-dependent manner (Figs. 3B and 4B, left; 3C and 4C, left). In addition, total perfusion in all speed regions was significantly lower on tumor skin compared with that in control skin, and P. Barbital treatment significantly improved total perfusion on tumor skin (Figs. 3D and 4D, left). Mean percentage of total perfusion for the three perfusion components was also compared; the results showed that mean percentage of total perfusion in low-speed region significantly increased on tumor skin compared with that in the control skin and that medium and high concentrations of P. Barbital stimulation led to a notable drop in mean percentage of total perfusion in low-speed region on tumor skin. Consistent with the findings on blood flux on tumor skin, P. Barbital treatment also significantly increased the blood flux in the mid- and high-speed regions and total perfusion in all speed regions on tumor surface (Ts) in a dose-dependent manner (Figs. 3B and 4B, right; 3C and 4C, right). However, there was a slightly different impact of P. Barbital on blood flux in low-speed regions (<1 mm/s) between Sk and Ts, as shown in Figs. 3A and 4A. P. Barbital increased blood flux in low-speed regions (<1 mm/s) on tumor surface in a dose-dependent manner.

Taken together, these data suggest that 50 mg/kg P. Barbital is effective enough to reduce blood perfusion in nutritive capillaries with low-speed flow on tumor skin and that P. Barbital has excellent efficacy in increasing blood perfusion in larger microvascular vessels with high-speed flow on tumor skin in a dose-dependent manner. P. Barbital stimulation led to an elevated blood flux in all three speed regions on tumor surface.

Effect of Sodium Pentobarbital on Oxyhemoglobin Saturation, Tissue Concentration of Total Hemoglobin, and RBC Tissue Fraction on Tumor Skin and Tumor Surface. Tumoral metabolic measurements such as tissue concentrations of oxygenized hemoglobin (ctO_2Hb), deoxygenized hemoglobin (ctHHb), total hemoglobin (ctTHb), and oxyhemoglobin saturation (SO_2) are directly associated with tumor metabolism and vascular features. The difference between tumors and healthy tissue is expected to be achieved by comparing ctTHb and SO_2; thus, in the present study, we investigated whether P. Barbital had an effect on SO_2 and ctTHb in both tumor skin and tumor surface. Quantitative analysis revealed a notable reduction in SO_2 on tumor skin compared with the normal skin (38.77% vs. 52.19%, $P < 0.0001$), and low dose (5 mg/kg) P. Barbital treatment resulted in a moderate increase in SO_2 on tumor skin compared with untreated tumors (40.3% vs. 38.77%, $P = 0.017$; Figs. 5A and 6A). Interestingly, mid- and high-dose (25 mg/kg and 50 mg/kg) P. Barbital treatment further reduced SO_2 on tumor skin when compared with untreated tumors. Consistently, low dose P. Barbital exposure also mildly increased SO_2 on tumor surface compared with untreated tumor surface (50.1% vs. 48.6%, $P = 0.0048$), and mid- and high-dose P. Barbital treatment further decreased SO_2 on tumor surface (44.69% vs. 42.49% vs. 48.6%, both $P < 0.0001$; Figs. 5B and 6B). Furthermore, tumor skin exhibited significant raise of ctTHb compared with control skin (16.81 μM vs. 10.13 μM, $P < 0.0001$), and mid- and high-level P. Barbital exposure reduced ctTHb on tumor skin to normal level compared with the skin of untreated tumors (7.95 μM vs. 9.69 μM vs. 16.81 μM, both $P < 0.0001$; Figs. 5C and 6C). Similarly, P. Barbital treatment significantly decreased ctTHb on tumor surface when compared with untreated tumor surface at a dose-dependent manner (35.39 μM vs. 31.79 μM vs. 22.37 μM vs. 39.9 μM; Figs. 5D and 6D). In the present study, we also assessed the effect of different doses of P. Barbital treatment on RBC tissue fraction on tumor skin and tumor surface. As shown in Figs. 5E and 6E, RBC tissue fraction was much higher on tumor skin compared with control skin (0.33% vs. 0.19%) and application of low dose P. Barbital further increased the RBC tissue fraction. Instead, mid- and high-dose P. Barbital exposure significantly reduced RBC tissue fraction on tumor skin compared with

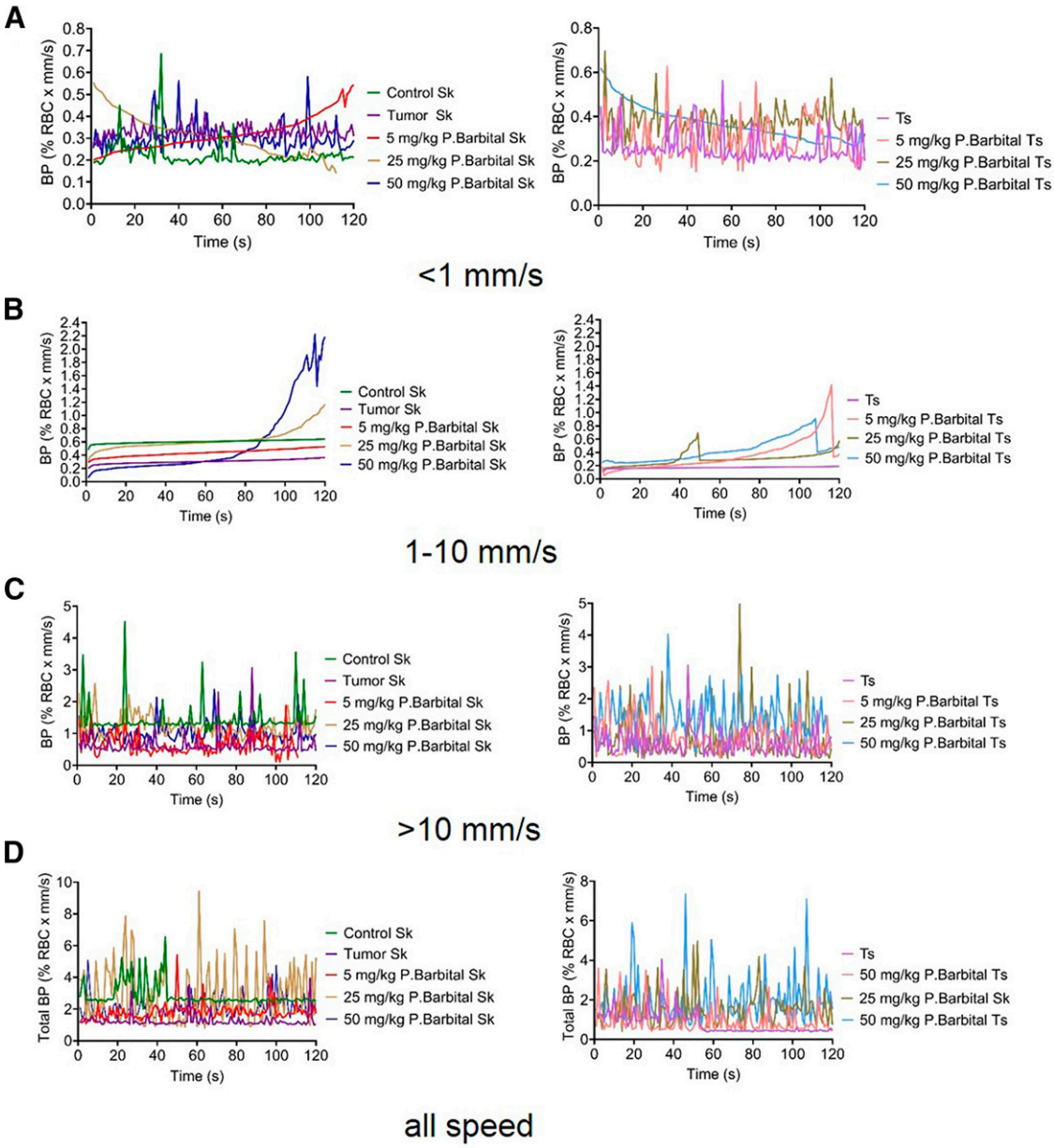

Fig. 3. Effects of sodium pentobarbital on blood perfusion on both tumor skin (Sk) and tumor surface (Ts) as presented with line charts. Blood perfusion in % RBC times their speed [divided into speed regions of 0–1 mm/s (A), 1–10 mm/s (B), and above 10 mm/s (C)] and total perfusion (D) on both Sk (left) and Ts (right) were shown in different groups: control, tumor, and 5, 25, and 50 mg/kg P. Barbital groups.

untreated tumors (0.19% vs. 0.15% vs. 0.33%). The same phenomenon occurred on tumor surface, as Figs. 5F and 6F presented; low dose P. Barbital treatment caused elevated RBC tissue fraction on tumor surface compared with untreated tumors, and application of high dose P. Barbital resulted in a significant drop in RBC tissue fraction on tumor surface when compared with untreated tumors. Collectively, these results revealed the opposite effect of different doses of P. Barbital on ctO_2Hb, ctTHb, and RBC tissue fraction on both tumor skin and tumor surface.

Discussion

In the present study, we observed that 1) P. Barbital suppressed breast tumor growth both in vitro and in vivo; 2) high dose (50 mg/kg) P. Barbital treatment cause a significant reduction in blood flux in nutritive capillaries with low-speed flow on tumor skin, whereas P. Barbital consumption resulted in an increased blood flux in larger micro vessels with high-speed flow in a dose-dependent manner; P. Barbital treatment led to an elevated blood flux in all three speed regions on tumor surface; and 3) different doses of P. Barbital play distinct roles in ctO_2Hb, ctTHb, and RBC tissue fraction on both tumor skin and tumor surface. The method used in this study provides data in absolute units rather than presenting microcirculatory parameters in arbitrary units as in many previous literatures.

Heterogeneity of tumors including breast cancer is the principal cause of acquired treatment resistance, recurrence, and progression (Polyak, 2011; Zardavas et al., 2015; AlSendi et al., 2021; Skowron et al., 2021). Reducing treatment-related side effects is another major challenge

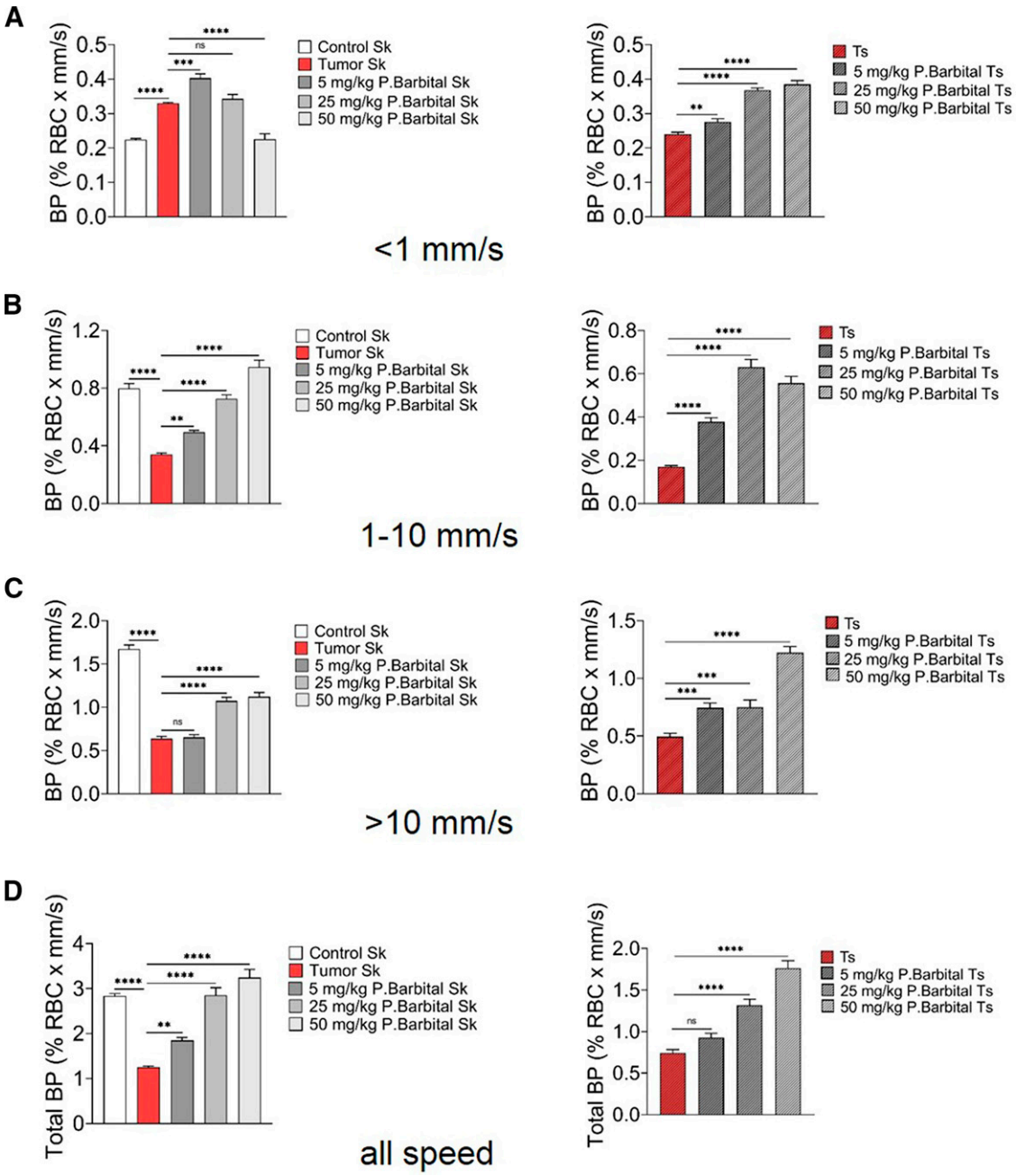

Fig. 4. Different influences of sodium pentobarbital on blood perfusion for three speed regions on both tumor skin and tumor surface. Blood perfusion for low-speed region (0 to 1 mm/s) (A), mid-speed region (1–10 mm/s) (B), and high-speed region (>10 mm/s) on skin (Sk, left) and tumor surface (Ts, right) was evaluated by using EPOS system in tumor-bearing mice treated with different doses of sodium pentobarbital and healthy controls. Data are presented as the mean ± S.D. ****$P \leq 0.0001$; ***P ≤ 0.001; **$P \leq 0.01$.

for clinicians (Berliere et al., 2021). Effective drugs or adjuvant drugs for breast cancer with fewer adverse effects are currently still being explored.

Sodium pentobarbital, a short-acting GABAA-receptor potentiator, which is usually used as a preoperative anesthetic in severe insomnia and seizure epilepsy emergency management, can cause a loss of consciousness and cardiovascular depression (Olsen and Li, 2011; Priest and Geisbuhler, 2015; Sierra-Valdez et al., 2016). A study from Xie et al. (2009) showed that anesthetic pentobarbital was capable of suppressing proliferation and migration of C6 malignant glioma cells in a concentration-dependent manner. Anesthetic sevoflurane was also shown to exert antiproliferative and antimetastatic effects on osteosarcoma cells by inactivating PI3K/AKT pathway (Gao et al., 2019). In accordance with these findings, in this study we demonstrated that sodium pentobarbital significantly inhibited the growth of breast cancer in a dose-dependent manner both in vitro and in vivo. In addition, the doses of sodium pentobarbital used in the current experiment (under 50 mg/kg in animal model) are safe and reliable and are not associated with obvious side effects.

In the current study, we examined the differences of cutaneous microcirculatory parameters between tumor-bearing mice

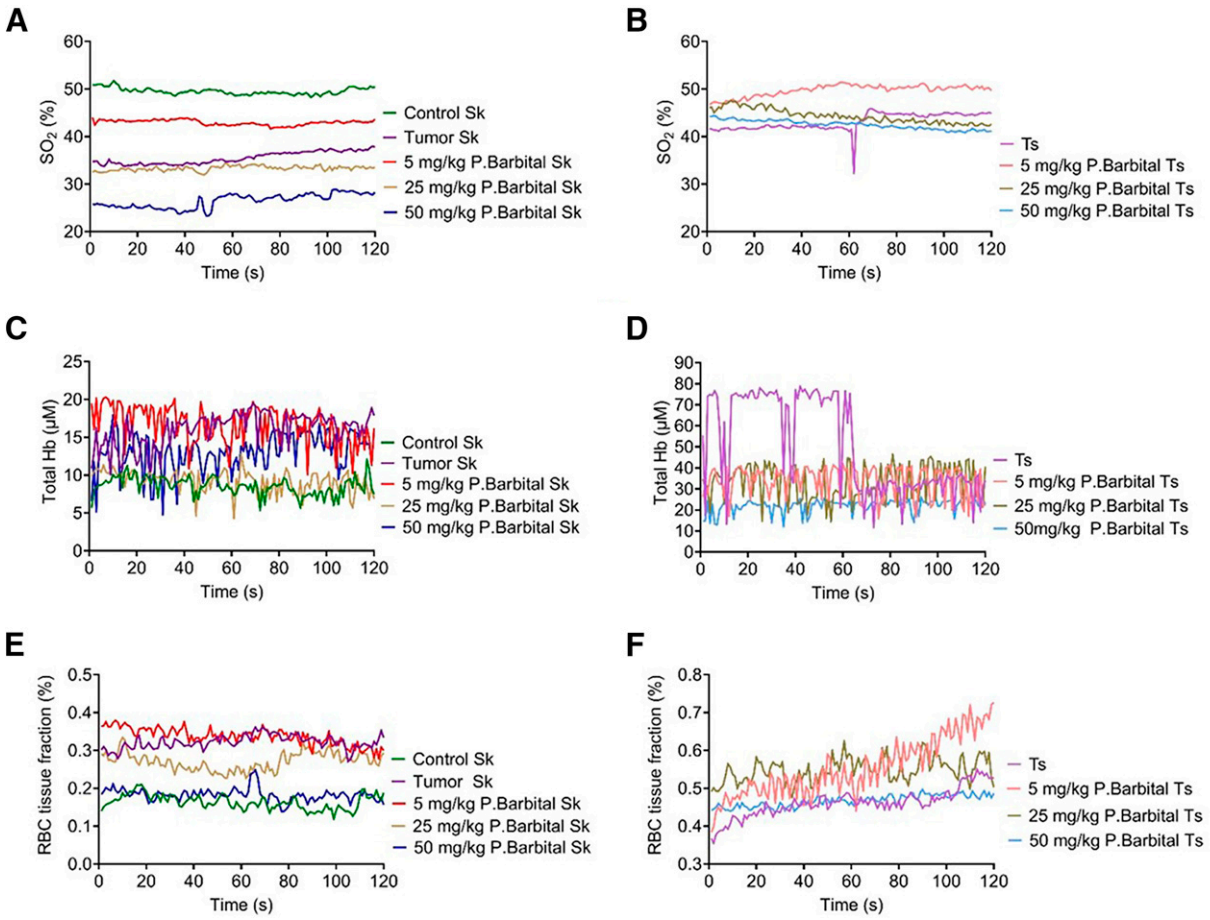

Fig. 5. Effects of sodium pentobarbital on oxygenation on both tumor skin (Sk) and tumor surface (Ts) as presented with line charts. Oxyhemoglobin saturation (SO_2) (A and B), tissue concentration of total hemoglobin (ctTHb) (C and D), and red blood cell (RBC) tissue fraction (E and F) on both Sk (A, C, and E) and Ts (B, D, and F) in different groups: control, tumor, and 5, 25, and 50 mg/kg P. Barbital groups are shown by line charts.

and healthy mice and assessed the influences of sodium pentobarbital on cutaneous microcirculation. We employed a new LDF signal analysis, which enables separating the blood flow into three flow speed regions to correlate differences in the speed distribution to specific vessel types, as large vessels such as arterioles, venules, and arteriovenous shunts are commonly associated with higher blood flow velocity than smaller vessels, which are mainly nutritive capillaries (Fredriksson et al., 2010). We have shown that the elevated blood perfusion occurred in vessels with a velocity <1 mm/s on tumor skin due to higher metabolic demand when compared with the control skin and that high dose (50 mg/kg) P. Barbital treatment attenuated the increased blood perfusion for low-speed region on tumor skin, suggesting an inhibiting role for high dose of P. Barbital. These results were consistent with the findings by Pedanekar et al. (2019), who have revealed a notable decrease in the blood flux on the skin surface along with the smaller tumor size in patients with good therapeutic response. Similarly, the highest level of skin blood flow has been observed in patients with breast cancer compared with benign breast and healthy controls (Seifalian et al., 1995). On the contrary, a significant reduction of blood perfusion was observed in larger vessels with mid and high speed on tumor skin, and P. Barbital treatment increased the blood perfusion for mid- and high-speed regions on tumor skin. These results can be explained at least partially by the fact that ?the? larger vessels with high-speed perfusion were crucial to the endothelial function; under some pathologic conditions such as diabetes, endothelial injury occurred, resulting in inhibition of nitric oxide (NO)-mediated vasodilation and reduction of high-speed perfusion (Bergstrand et al., 2018). P. Barbital can increase the blood perfusion for mid- and high-speed regions on tumor skin in a dose-dependent manner.

With regard to blood perfusion on tumor surface, our findings indicated that P. Barbital markedly increased the blood perfusion for all three speed regions compared with untreated tumors. These findings were consistent with previous study, which indicated that low tumor blood flow could be a crucial feature of rectal cancer aggressiveness and that higher tumor blood flow was a predictor of good neoadjuvant treatment response (Bakke et al., 2020). The underlying mechanism for the above findings may be related to the fact that tumor angiogenesis is extraordinarily active, leading to abnormal vascular structure including tortuosity, dilation and inadequate pericyte coverage, and subsequent vascular dysfunction including insufficient blood flow. P. Barbital treatment can normalize tumor vasculature and then increase blood perfusion in tumor tissue. However, Vaupel and Kelleher, 2013 have shown that the overall mean flow in prostate cancer (PC) tissue is

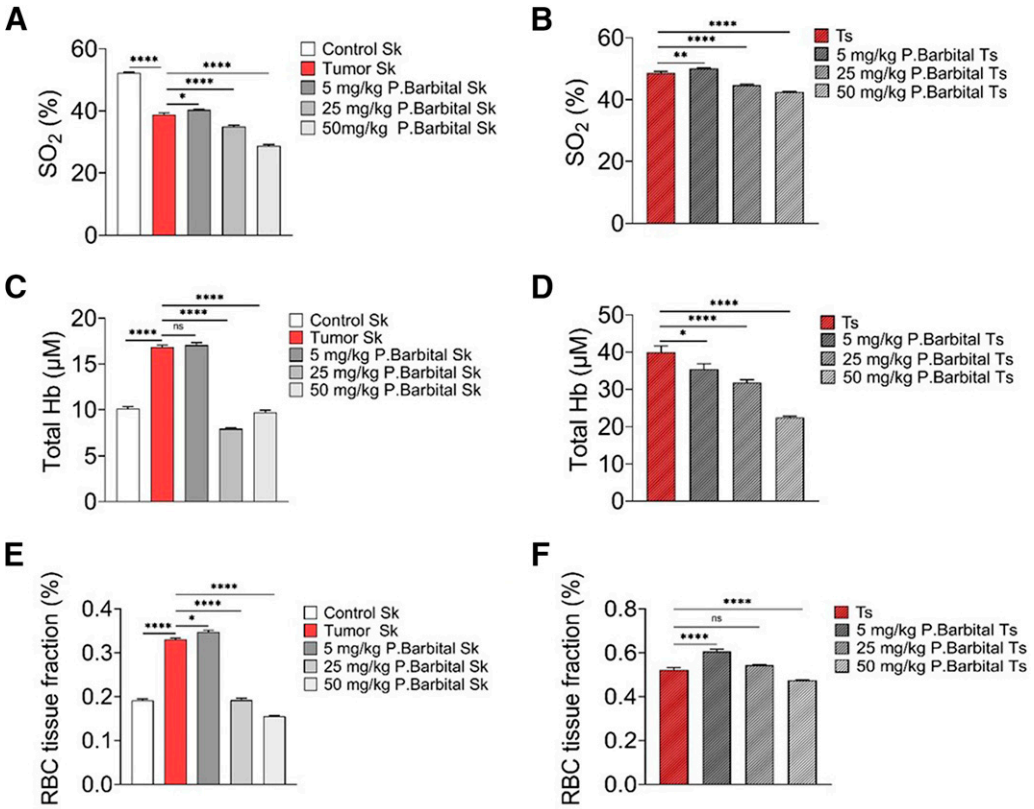

Fig. 6. Different concentrations of sodium pentobarbital have different roles on oxygenation on both skin and tumor surface. Oxyhemoglobin saturation (SO_2) (A), tissue concentration of total hemoglobin (ctTHb) (B), and red blood cell (RBC) tissue fraction (C) of tumor skin (Sk) and tumor surface (Ts) were monitored by using EPOS system in tumor-bearing mice treated with different doses of sodium pentobarbital and healthy controls. Data are presented as the mean ± S.D. $^{****}P \leq 0.0001$; $^{**}P \leq 0.01$; $^{*}P \leq 0.05$.

approximately three times higher than that in normal prostate (NP) tissue. The conflicting results are at least in part due to the difference in measurement positions (Vinik et al., 2001) and instrumentation (Fredriksson et al., 2009) used.

Tumoral tissue oxygen saturation (SO_2) has been considered as an early predictive factor of tumor response to treatment, and lower SO_2 is associated with noncomplete pathologic response to treatment (Ueda et al., 2012; Cochran et al., 2018). EPOS system in this study revealed a rise on tumor surface for SO_2 and a reduction in the concentration of total hemoglobin (ctTHb) after low-dose (5 mg/kg) P. Barbital therapy, and mid- and high-dose P. Barbital treatment further reduced ctTHb. Increased SO_2 represents less tumoral hypoxia, and decreased ctTHb indicates smaller blood volume of the tumors. Previous studies also demonstrated that mean ctTHb in breast tumors was about 3.5 times higher than that in normal counterpart due to larger blood volume and that ctTHb over SO_2 further distinguished between tumoral and normal breast tissue (Grosenick et al., 2005). Thus, tumor growth inhibition effect of P. Barbital is at least in part due to its role in decreasing ctTHb on tumor surface. Interestingly, in this study, we found that mid- and high-dose P. Barbital treatment further exacerbated the reduction in tumor SO_2, and the underlying mechanisms need to be further explored. To the best of our knowledge, this is the first study to assess the differences of cutaneous SO_2 and ctTHb between tumor-bearing and healthy mice. The SO_2 and ctTHb in cutaneous blood are thought to be strongly associated with cutaneous metabolism (Nagashima et al., 2000). In untreated tumor-bearing group, a decline of cutaneous SO_2 was observed, together with an increase in ctTHb compared with healthy controls. P. Barbital treatment resulted in a notable increase for cutaneous SO_2 in a dose-dependent manner, and mid- and high-dose P. Barbital therapy caused marked reduction for cutaneous ctTHb. Like SO_2, red blood cell (RBC) tissue fraction is a crucial parameter reflecting microvascular function (Ewerlöf et al., 2021). Moreover, quantifying blood flow, oxygenation, and RBC tissue fraction simultaneously from the same position of the tissue may offer an optimal assessment of the microcirculation under physiopathological conditions. However, as far as we know, there have been few studies estimating the association between RBC tissue fraction and microvascular function in diseases (Jonasson et al., 2017). In the present study, we observed the increased cutaneous RBC tissue fraction in tumor-bearing mice compared with healthy controls, and 5 mg/kg P. Barbital treatment caused further increase of RBC tissue fraction on both tumor skin and tumor surface. On the contrary, 25 mg/kg and 50 mg/kg P. Barbital therapy significantly reduced RBC tissue fraction on both tumor skin and tumor surface. Although EPOS system is a relatively new device, it uses diffuse reflectance spectroscopy (DRS), which is a not common optical method in recent years, to quantify the SO_2. The prominent feature of EPOS system is that it combines the DRS and laser Doppler flowmetry (LDF) into one joint model to increase the credibility of the method analyzing data from the two techniques separately.

This study has some limitations. Firstly, we observed the antitumor effect of P. Barbital on tumor growth and its role in regulating blood perfusion and oxygenation on both skin and tumor surface. However, the molecular mechanisms underlying these observations have not been explored in the present study and need to be further investigated. Secondly, whether P. Barbital has similar effects on other types of tumors also needs to be further studied. Thirdly, this study showed the opposite effects of P. Barbital on oxygen saturation and total hemoglobin on tumor skin; therefore, other technologies should be used to verify these effects in further studies.

In conclusion, we demonstrated the anticancer effect of P. Barbital. Firstly, P. Barbital suppresses breast tumor growth both in vitro and in vivo in a dose-dependent manner. Secondly, P. Barbital inhibited breast tumor growth at least partly through normalizing both cutaneous and tumor surface blood perfusion. Thirdly, different doses of P. Barbital play distinct roles in ctO_2Hb, ctTHb, and RBC tissue fraction on both tumor skin and tumor surface.

Acknowledgments

This work received help from Mingming Liu and Yuan Li, both of whom are from Institute of Microcirculation, Chinese Academy of Medical Sciences and Peking Union Medical College, in the use and maintenance of the EPOS system.

Authorship Contributions

Participated in research design: Wang, Zhang.

Conducted experiments: Wang, Liu, B. Li, Yang, Lu, A. Li, H. Li, Zhang, Han.

Performed data analysis: Wang, Liu, Zhang.

Wrote or contributed to the writing of the manuscript: Wang, Zhang, Han.

References

Agarwal SC, Allen J, Murray A, and Purcell IF (2012) Laser Doppler assessment of dermal circulatory changes in people with coronary artery disease. *Microvasc Res* **84**:55–59.

AlSendi M, O'Reilly D, Zeidan YH, and Kelly CM (2021) Oligometastatic breast cancer: are we there yet? *Int J Cancer* **149**:1520–1528.

Anderson ME, Moore TL, Lunt M, and Herrick AL (2004) Digital iontophoresis of vasoactive substances as measured by laser Doppler imaging–a non-invasive technique by which to measure microvascular dysfunction in Raynaud's phenomenon. *Rheumatology (Oxford)* **43**:986–991.

Andleeb F, Katta N, Gruslova A, Muralidharan B, Estrada A, McElroy AB, Ullah H, Brenner AJ, and Milner TE (2021) Differentiation of brain tumor microvasculature from normal vessels using optical coherence angiography. *Lasers Surg Med* **53**:1386–1394.

Bakke KM, Meltzer S, Grøvik E, Negård A, Holmedal SH, Gjesdal K-I, Bjørnerud A, Ree AH, and Redalen KR (2020) Sex differences and tumor blood flow from dynamic susceptibility contrast MRI are associated with treatment response after chemoradiation and long-term survival in rectal cancer. *Radiology* **297**:352–360.

Barry EF, O'Neill J, Abdulla MH, and Johns EJ (2021) The renal excretory responses to acute renal interstitial angiotensin (1-7) infusion in anaesthetised spontaneously hypertensive rats. *Clin Exp Pharmacol Physiol* **48**:1674–1684.

Bergstrand S, Morales M-A, Coppini G, Larsson M, and Strömberg T (2018) The relationship between forearm skin speed-resolved perfusion and oxygen saturation, and finger arterial pulsation amplitudes, as indirect measures of endothelial function. *Microcirculation* **25**:e12422.

Berliere M, Piette N, Bernard M, Lacroix C, Gerday A, Samartzi V, Coyette M, Roelants F, Docquier M-A, Touil N, et al. (2021) Hypnosis sedation reduces the duration of different side effects of cancer treatments in breast cancer patients receiving neoadjuvant chemotherapy. *Cancers (Basel)* **13**:4147.

Ciruelos E, Apellániz-Ruiz M, Cantos B, Martinez-Jáñez N, Bueno-Muiño C, Echarri M-J, Enrech S, Guerra J-A, Manso L, Pascual T, et al. (2019) A pilot, phase II, randomized, open-label clinical trial comparing the neurotoxicity of three dose regimens of nab-paclitaxel to that of solvent-based paclitaxel as the first-line treatment for patients with human epidermal growth factor receptor type 2-negative metastatic breast cancer. *Oncologist* **24**:e1024–e1033.

Cochran JM, Busch DR, Leproux A, Zhang Z, O'Sullivan TD, Cerussi AE, Carpenter PM, Mehta RS, Roblyer D, Yang W, et al. (2018) Tissue oxygen saturation predicts response to breast cancer neoadjuvant chemotherapy within 10 days of treatment. *J Biomed Opt* **24**:1–11.

Concistrè A, Petramala L, Bonvicini M, Gigante A, Collalti G, Pellicano C, Olmati F, Iannucci G, Soldini M, Rosato E, et al. (2020) Comparisons of skin microvascular changes in patients with primary aldosteronism and essential hypertension. *Hypertens Res* **43**:1222–1230.

Deegan AJ and Wang RK (2019) Microvascular imaging of the skin. *Phys Med Biol* **64**:07TR01.

Ewerlöf M, Salerud EG, Strömberg T, and Larsson M (2021) Estimation of skin microcirculatory hemoglobin oxygen saturation and red blood cell tissue fraction using a multispectral snapshot imaging system: a validation study. *J Biomed Opt* **26**:026002.

Feng W, Shi R, Zhang C, Liu S, Yu T, and Zhu D (2018) Visualization of skin microvascular dysfunction of type 1 diabetic mice using in vivo skin optical clearing method. *J Biomed Opt* **24**:1–9.

Fredriksson I, Burdakov O, Larsson M, and Strömberg T (2013) Inverse Monte Carlo in a multilayered tissue model: merging diffuse reflectance spectroscopy and laser Doppler flowmetry. *J Biomed Opt* **18**:127004.

Fredriksson I, Larsson M, Nyström FH, Länne T, Ostgren CJ, and Strömberg T (2010) Reduced arteriovenous shunting capacity after local heating and redistribution of baseline skin blood flow in type 2 diabetes assessed with velocity-resolved quantitative laser Doppler flowmetry. *Diabetes* **59**:1578–1584.

Fredriksson I, Larsson M, and Strömberg T (2009) Measurement depth and volume in laser Doppler flowmetry. *Microvasc Res* **78**:4–13.

Gao K, Su Z, Liu H, and Liu Y (2019) Anti-proliferation and anti-metastatic effects of sevoflurane on human osteosarcoma U2OS and Saos-2 cells. *Exp Mol Pathol* **108**:121–130.

Grosenick D, Wabnitz H, Moesta KT, Mucke J, Schlag PM, and Rinneberg H (2005) Time-domain scanning optical mammography: II. Optical properties and tissue parameters of 87 carcinomas. *Phys Med Biol* **50**:2451–2468.

Harrison CA, Parks RM, and Cheung KL (2021) The impact of breast cancer surgery on functional status in older women - a systematic review of the literature. *Eur J Surg Oncol* **47**:1891–1899.

Hsiu H, Chen C-T, Hung S-H, Chen G-Z, and Huang Y-L (2018) Differences in time-domain and spectral indexes of skin-surface laser-Doppler signals between controls and breast-cancer subjects. *Clin Hemorheol Microcirc* **69**:371–381.

Ilhan E, Chee E, Hush J, and Moloney N (2017) The prevalence of neuropathic pain is high after treatment for breast cancer: a systematic review. *Pain* **158**:2082–2091.

Jing X, Yang F, Shao C, Wei K, Xie M, Shen H, and Shu Y (2019) Role of hypoxia in cancer therapy by regulating the tumor microenvironment. *Mol Cancer* **18**:157.

Jonasson H, Bergstrand S, Nystrom FH, Länne T, Östgren CJ, Bjarnegård N, Fredriksson I, Larsson M, and Strömberg T (2017) Skin microvascular endothelial dysfunction is associated with type 2 diabetes independently of microalbuminuria and arterial stiffness. *Diab Vasc Dis Res* **14**:363–371.

Jonasson H, Fredriksson I, Larsson M, and Strömberg T (2019) Validation of speed-resolved laser Doppler perfusion in a multimodal optical system using a blood-flow phantom. *J Biomed Opt* **24**:1–8.

Jonasson H, Fredriksson I, Pettersson A, Larsson M, and Strömberg T (2015) Oxygen saturation, red blood cell tissue fraction and speed resolved perfusion - a new optical method for microcirculatory assessment. *Microvasc Res* **102**:70–77.

Koch KU, Mikkelsen IK, Aanerud J, Espelund US, Tietze A, Oettingen GV, Juul N, Nikolajsen L, Østergaard L, and Rasmussen M (2020) Ephedrine versus phenylephrine effect on cerebral blood flow and oxygen consumption in anesthetized brain tumor patients: a randomized clinical trial. *Anesthesiology* **133**:304–317.

Matsuura S and Downie JW (2000) Effect of anesthetics on reflex micturition in the chronic cannula-implanted rat. *Neurourol Urodyn* **19**:87–99.

Miller JW, Ding L, Gunter JB, Lam JE, Lin EP, Paquin JR, Li BL, Spaeth JP, Kreeger RN, Divanovic A, et al. (2018) Comparison of intranasal dexmedetomidine and oral pentobarbital sedation for transthoracic echocardiography in infants and toddlers: a prospective, randomized, double-blind trial. *Anesth Analg* **126**:2009–2016.

Mohamed AS, Hosney M, Bassiony H, Hassanein SS, Soliman AM, Fahmy SR, and Gaafar K (2020) Sodium pentobarbital dosages for exsanguination affect biochemical, molecular and histological measurements in rats. *Sci Rep* **10**:378.

Nagashima Y, Yada Y, Hattori M, and Sakai A (2000) Development of a new instrument to measure oxygen saturation and total hemoglobin volume in local skin by near-infrared spectroscopy and its clinical application. *Int J Biometeorol* **44**:11–19.

Naito M, Aoyama H, and Ito A (1985) Inhibitory effect of phenobarbital on the development of gliomas in WF rats treated neonatally with N-ethyl-N-nitrosourea. *J Natl Cancer Inst* **74**:725–728.

National Research Council (US) Committee for the Update of the Guide for the Care and Use of Laboratory Animals (2011) *Guide for the Care and Use of Laboratory Animals*, 8th ed, National Academies Press, Washington, DC.

Olsen RW and Li G-D (2011) GABA(A) receptors as molecular targets of general anesthetics: identification of binding sites provides clues to allosteric modulation. *Can J Anaesth* **58**:206–215.

Park SB, Goldstein D, Krishnan AV, Lin CS, Friedlander ML, Cassidy J, Koltzenburg M, and Kiernan MC (2013) Chemotherapy-induced peripheral neurotoxicity: a critical analysis. *CA Cancer J Clin* **63**:419–437.

Pedanekar T, Kedare R, and Sengupta A (2019) Monitoring tumor progression by mapping skin microcirculation with laser Doppler flowmetry. *Lasers Med Sci* **34**:61–77.

Polyak K (2011) Heterogeneity in breast cancer. *J Clin Invest* **121**:3786–3788.

Priest SM and Geisbuhler TP (2015) Injectable sodium pentobarbital: stability at room temperature. *J Pharmacol Toxicol Methods* **76**:38–42.

Roustit M and Cracowski J-L (2012) Non-invasive assessment of skin microvascular function in humans: an insight into methods. *Microcirculation* **19**:47–64.

Sang X, Li L, Rui C, Liu Y, Liu Z, Tao Z, Cheng H, and Liu P (2021) Induction of EnR stress by melatonin enhances the cytotoxic effect of lapatinib in HER2-positive breast cancer. *Cancer Lett* **518**:82–93.

Savard M-F, Clemons M, Hutton B, Jemaan Alzahrani M, Caudrelier J-M, Vandermeer L, Liu M, Saunders D, Sienkiewicz M, Stober C, et al. (2021) De-escalating adjuvant therapies in older patients with lower risk estrogen receptor-positive breast cancer

treated with breast-conserving surgery: a systematic review and meta-analysis. *Cancer Treat Rev* **99**:102254.
Seifalian AM, Chaloupka K, and Parbhoo SP (1995) Laser Doppler perfusion imaging–a new technique for measuring breast skin blood flow. *Int J Microcirc Clin Exp* **15**:125–130.
Shamim-Uzzaman QA, Pfenninger D, Kehrer C, Chakrabarti A, Kacirotti N, Rubenfire M, Brook R, and Rajagopalan S (2002) Altered cutaneous microvascular responses to reactive hyperaemia in coronary artery disease: a comparative study with conduit vessel responses. *Clin Sci (Lond)* **103**:267–273.
Sierra-Valdez FJ, Ruiz-Suárez JC, and Delint-Ramirez I (2016) Pentobarbital modifies the lipid raft-protein interaction: a first clue about the anesthesia mechanism on NMDA and GABAA receptors. *Biochim Biophys Acta* **1858**:2603–2610.
Skowron MA, Oing C, Bremmer F, Ströbel P, Murray MJ, Coleman N, Amatruda JF, Honecker F, Bokemeyer C, Albers P, et al. (2021) The developmental origin of cancers defines basic principles of cisplatin resistance. *Cancer Lett* **519**:199–210.
Smith KJ, Argarini R, Carter HH, Quirk BC, Haynes A, Naylor LH, McKirdy H, Kirk RW, McLaughlin RA, and Green DJ (2019) Novel noninvasive assessment of microvascular structure and function in humans. *Med Sci Sports Exerc* **51**:1558–1565.
Sung H, Ferlay J, Siegel RL, Laversanne M, Soerjomataram I, Jemal A, and Bray F (2021) Global cancer statistics 2020: GLOBOCAN estimates of incidence and mortality worldwide for 36 cancers in 185 countries. *CA Cancer J Clin* **71**:209–249.
Tanioka M, Park WK, Park J, Lee JE, and Lee BH (2020) Lipid emulsion improves functional recovery in an animal model of stroke. *Int J Mol Sci* **21**:7373.
Tromberg BJ, Zhang Z, Leproux A, O'Sullivan TD, Cerussi AE, Carpenter PM, Mehta RS, Roblyer D, Yang W, Paulsen KD, et al.; ACRIN 6691 Investigators (2016) Predicting responses to neoadjuvant chemotherapy in breast cancer: ACRIN 6691 trial of diffuse optical spectroscopic imaging. *Cancer Res* **76**:5933–5944.
Ueda S, Roblyer D, Cerussi A, Durkin A, Leproux A, Santoro Y, Xu S, O'Sullivan TD, Hsiang D, Mehta R, et al. (2012) Baseline tumor oxygen saturation correlates with a pathologic complete response in breast cancer patients undergoing neoadjuvant chemotherapy. *Cancer Res* **72**:4318–4328.
Vaupel P and Kelleher DK (2013) Blood flow and oxygenation status of prostate cancers. *Adv Exp Med Biol* **765**:299–305.
Vinik AI, Erbas T, Park TS, Pierce KK, and Stansberry KB (2001) Methods for evaluation of peripheral neurovascular dysfunction. *Diabetes Technol Ther* **3**:29–50.
Warden CN, Bernard PK, and Kimball TR (2010) The efficacy and safety of oral pentobarbital sedation in pediatric echocardiography. *J Am Soc Echocardiogr* **23**:33–37.
Xie J, Li Y, Huang Y, Qiu P, Shu M, Zhu W, Ou Y, and Yan G (2009) Anesthetic pentobarbital inhibits proliferation and migration of malignant glioma cells. *Cancer Lett* **282**:35–42.
Xu S-F, Du G-H, Abulikim K, Cao P, and Tan H-B (2020) Verification and defined dosage of sodium pentobarbital for a urodynamic study in the possibility of survival experiments in female rat. *BioMed Res Int* **2020**:6109497.
Zardavas D, Irrthum A, Swanton C, and Piccart M (2015) Clinical management of breast cancer heterogeneity. *Nat Rev Clin Oncol* **12**:381–394.

Address correspondence to: Jianqun Han, Microhemodynamics Laboratory, Institute of Microcirculation, Chinese Academy of Medical Sciences and Peking Union Medical College, Dong Dan San Tiao 5 Hao, Dongcheng District, Beijing 100005, China. E-mail: jianqunhan123456@163.com; or Xiaoyan Zhang, Laboratory of Microvascular Biopathology, Institute of Microcirculation, Chinese Academy of Medical Sciences and Peking Union Medical College, Dong Dan San Tiao 5 Hao, Dongcheng District, Beijing 100005, China. E-mail: xiaoyan111666@sina.com